A vascular-liver chip for sensitive detection of nutraceutical metabolites from human pluripotent stem cell derivatives

Fang Yu,[1,2] Yeek Teck Goh,[3,4] Huan Li,[1] Narmada Balakrishnan Chakrapani,[3] Ming Ni,[5] Guo Lin Xu,[1,6] Tseng-Ming Hsieh,[1,6] Yi-Chin Toh,[7,8,9] Christine Cheung,[3,10] Ciprian Iliescu,[1,11,a)] and Hanry Yu[1,12,13,14,b)]

AFFILIATIONS

[1]Institute of Bioengineering and Nanotechnology, A*STAR, The Nanos, #04-01, 31 Biopolis Way, Singapore 138669
[2]Singapore Institute of Manufacturing Technology, A*STAR, 2 Fusionopolis Way, #08-04, Innovis, Singapore 138634
[3]Institute of Molecular and Cell Biology, A*STAR, Proteos, 61 Biopolis Drive, Singapore 138673
[4]Genome Institute of Singapore, A*STAR, Genome, 60 Biopolis Street, Singapore 138672
[5]School of Biological Sciences and Engineering, Yachay Tech University, Hacienda San José s/n, San Miguel de Urcuquí 100105, Ecuador
[6]NanoBio Lab, A*STAR, The Nanos, #09-01 31 Biopolis Way, Singapore 138669
[7]Department of Biomedical Engineering, National University of Singapore, 4 Engineering Drive 3, Singapore 117583
[8]Queensland University of Technology, School of Mechanical, Medical and Process Engineering, Garden Point Campus, Brisbane, QLD 4000, Australia
[9]Queensland University of Technology, Institute of Health and Biomedical Innovation, 60 Musk Ave, Kelvin Grove, QLD 4059, Australia
[10]Lee Kong Chian School of Medicine, Nanyang Technological University Singapore, 59 Nanyang Drive, Singapore 636921
[11]National Institute for Research and Development in Microtechnologies, IMT-Bucharest, Bucharest 077190, Romania
[12]Mechanobiology Institute, National University of Singapore, T-Lab, 5A Engineering Drive 1, Singapore 117411
[13]Department of Physiology, National University of Singapore, MD9 #03-03, 2 Medical Drive, Singapore 117597
[14]Singapore-MIT Alliance for Research and Technology, 1 CREATE Way, #10-01 CREATE Tower, Singapore 138602

[a)]**Author to whom correspondence should be addressed:** cipi_sil@yahoo.com
[b)]**E-mail:** nmiyuh@nus.edu.sg

ABSTRACT

Human pluripotent stem cell (hPSC) is a great resource for generating cell derivatives for drug efficiency testing. Metabolites of nutraceuticals can exert anti-inflammatory effects on blood vessels. However, the concentration of nutraceutical metabolites produced in hPSC-derived hepatocytes (hPSC-HEPs) is usually low. To enable the detection of these metabolites under the *in vitro* environment, we have developed a co-culture model consisting of parallel co-culture chambers and a recirculating microfluidic system with minimum fluid volume, optimal cell culture environment. The model allows cells to be exposed continuously to nutraceutical metabolites. In this perfused culturing model, hPSC-derived endothelial cells and hPSC-HEPs are co-cultured without physical contact. When an anti-inflammatory nutraceutical, quercetin, was administrated to the co-culture, higher levels of quercetin metabolites were detected on-chip compared with static control. We further induced inflammation with Interleukin-1β in the co-culture model and measured interleukin 8 (IL-8) generation. The IL-8 level was suppressed more significantly by quercetin metabolites in the perfusion co-culture, as compared to static culture. This is due to enhanced metabolites production on-chip. This microfluidic co-culture model enables *in vitro* screening of nutraceuticals using hPSC-derived cells.

Published under license by AIP Publishing. https://doi.org/10.1063/5.0004286

INTRODUCTION

Cardiovascular diseases are one leading cause of death (globally, 17.3 million deaths in 2013) and created significant healthcare burdens.[1] High blood pressure and high blood cholesterol are among the top risk factors.[2] Cardiovascular diseases such as coronary artery disease, stroke, and peripheral artery disease typically involve atherosclerosis. It is characterized by the thickening of the artery wall as a result of fibro-fatty plaque build-up. Atherosclerosis is caused by an interplay of inflammation involving multiple cell types.[3] Treatment of atherosclerosis usually requires long-term medications such as cholesterol-lowering statins, which have potential side effects.[4] In this direction, medical nutrition or nutraceuticals can help to prevent and to alleviate chronic cardiovascular diseases with minimum side effects.[5] Dietary nutrients and herbal extracts have been explored as nutraceuticals to treat atherosclerosis.[6,7] Due to their structural complexity, nutraceutical efficacy is usually harder to be predicted in preclinical screenings than small molecule drugs. A key organ involved in nutraceutical biotransformation is the liver, where compounds are metabolized to species with therapeutic or toxic effects.[8] Nutraceuticals are often metabolized in the liver into bioactive metabolites before they exhibit significant anti-inflammatory effects in the blood vessels. As a result, nutraceutical screening requires a human-relevant model that incorporates both vascular and liver components.

A cellular model with metabolic competencies is the foundation to investigate nutraceutical biotransformation. Human hepatocytes and endothelial cells are the most appropriate for this purpose. However, primary human hepatocytes are scarce and expensive, and this is a major limiting factor for their use in drug screening.[9] As an alternative cell source, human pluripotent stem cells (hPSC) can be differentiated into many cell types consistently and indefinitely.[10,11] Vascular[12,13] and hepatic[14] cells generated from hPSC have exhibited their respective tissue-specific phenotypes and functions. We have previously created hPSC-derived endothelial cells (hPSC-EC) capable of modeling atherosclerosis that responds to inflammatory stimulation[15] as well as hPSC-derived hepatocytes (hPSC-HEP) that show cytochrome P450 expression and respond to hepatotoxic drugs.[16] We have validated a static vascular-liver co-culture model as a platform for the efficacy testing of complex compounds.[17]

In recent years, the concept of organ-on-a-chip has generated a great deal of research interest because of its ability to simulate organ-level physiology. Organ-on-a-chip devices recapitulate the physicochemical microenvironment, tissue–tissue interface, and fluid flow in the body.[18–24] This makes it more ideal for studying complex organ functionalities than traditional 2D and 3D cell culture systems. Organ-on-a-chip systems connect several tissue types through microfluidic channels. A common culture medium is perfused through the systems for cell culture and drug testing.[25–29] Recirculation of media allows metabolites generated from drugs to be transported from one tissue chamber to another. This allows efficacies and toxicities of drugs and their metabolites to be predicted.[30–34] Despite their potential usefulness, organ-on-a-chip devices often have reduced molecular crosstalks because of limited cell count inside the devices as well as significant dilution of metabolic compounds due to media perfusion.[35] As a result, the effectiveness of drug exposure dosage in these systems is much smaller than static models and metabolites are more diluted and harder to detect. Moreover, for non-primary cell sources with lower metabolic functions such as hPSCs and induced pluripotent stem cells (iPSCs), it is important to have a cell culture platform with good drug testing sensitivity. Although it is very challenging to fully capture the complex drug metabolism which involves organ-level interactions in multiple tissue types, we aim to demonstrate that our co-culture perfusion chip model outperforms the conventional static culture platform for the testing of nutraceuticals. We intend to tackle these limitations of the current organ-on-a-chip system by engineering it to be suitable for testing complex compounds, such as nutraceuticals with multiple active metabolites.

Here, we report a vascular-liver co-culture model for nutraceutical metabolism studies using a perfusion incubator chip (PIC) which we developed in a previous study.[36] The co-culture model consists of a parallel culturing chamber that accommodates both the hPSC-derived vascular cells (on the top) and 3D hepatocytes (hPSC-HEP) spheroids (on the bottom). To increase metabolite concentration in the system, the culture medium was recirculated using a compact microfluidic circuit with a small total volume (3 ml). Moreover, to avoid the absorption of the drug and metabolites in the microfluidic chambers, hydrophilic materials were used in the microfluidic system. The constrained spheroid model was used for the hPSC-HEP to mimic liver organ functions in vitro.[36,37] We modified the polydimethylsiloxane (PDMS) surface with 3,4-dihydroxy-L-phenylalanine (DOPA) coating for better attachment of hPSC-EC under perfusion. Under perfusion condition, hPSC-EC showed increased metabolic activity. The PIC system improves both hPSC-EC and hPSC-HEP functions, allowing hPSC-HEPs to effectively transform quercetin into its active metabolites. We detected higher metabolites concentration in the perfusion culture compared with static culture. Quercetin's anti-inflammatory effects are more significant in perfusion co-culture model than in static co-culture (previously demonstrated in Ref. 17), thus making the system suitable for studying nutraceutical metabolism and predicting nutraceutical efficacies in vitro.

MATERIALS AND METHODS

hPSC-EC and hPSC-HEP generation and culture

hPSC-ECs are generated according to the protocols described in Ref. 17. Briefly, hPSC was first induced to undergo early mesoderm differentiation for 36 h, using a chemical defined media, supplemented with human recombinant FGF2 (20 ng/ml, R&D Systems), LY294002 (10 μM, Sigma), and human recombinant BMP4 (10 ng/ml, R&D Systems). Subsequently, lateral plate mesoderm was induced for 3.5 days, in media supplemented with human recombinant FGF2 (20 ng/ml) and BMP4 (50 ng/ml), with media change every 2 days. The mesoderm population was then trypsinized and plated on matrigel-coated cell culture plates in the same basal media supplemented with FGF2 (4 ng/ml), SB431542 (10 μM), and VEGF (50 ng/ml, R&D Systems), with media change every 2–3 days until day 10. After selection by fluorescence-activated cell sorting (FACS), cells expressing PECAM1 are plated at 2.6×10^5 cells/cm^2 onto collagen I-coated plates. The resulting hPSC-ECs are cultured in EGM-2 media (Lonza, Singapore) and were passaged with TrypLE Express (Gibco, USA) when 75% confluent.

hPSC-HEPs are generated using a growth factor-based differentiation protocol.[16] Differentiation was induced by a series of growth factors supplemented in the differentiation medium during a 20-day differentiation process. After differentiation, the cells were harvested using a serial 2× TrypLE Express treatment and dissociated into single cells using cell strainers. The single cells were then seeded to well plates coated with collagen I (50 μg/ml, Biolaboratories, Singapore). The hPSC-HEPs are maintained in Williams E medium (Sigma, Singapore). Attachment and recovery were promoted by culturing in step IV differentiation medium with Hepatocyte growth factor (R&D), Follistatin (R&D), Oncostatin (R&D) and Y-25632 (Rock Inhibitor).

Microfluidic chip setup

The structure and fabrication process of the perfusion incubator chip (PIC) was described in Ref. 36 (rat hepatocytes cell culture). Here, we underline the main elements and the modifications performed for the accommodation of the co-culture. The microfluidic system contains two glass reservoirs and two segments of stainless steel tubing [Fig. 1(a)]. The choice of stainless steel

tubing was motivated by its low drug absorption property and excellent hydrophilicity.[38] We limited the length of the tubing at 7 cm to reduce the total medium volume. This concentrates the metabolites and limits the amount of nutraceuticals absorbed into the tubing. The microfluidic chip composed of a rigid glass/silicon structure and a polydimethylsiloxane (PDMS)/glass structure. The glass/silicon structure contains the cell culture chamber, the microfluidic circuits, and an integrated heater. The PDMS and glass structure seals the chip and serves as a cell seeding substrate for hPSC-EC. The depth of the hPSC-EC seeding chamber was 300 μm while its diameter was 12 mm.

A cross section of the cell culture chamber is presented in Fig. 1(b). Silicone tubing (Cole-Parmer, USA) was used as a comparison. Chips and tubing were sterilized with 70% ethanol. 1 g/l bovine serum albumin (BSA) was used to prime the system.[39]

Driven by pressurized gas with 5% CO_2 (for maintaining the pH of the media), the flow rate in the system was set at 0.1 ml/h. The pressurized gas is connected to two bidirectional switches that control the flow direction [Fig. 1(c)]. The flow direction changes every 4 h to ensure adequate time for mass transfer and biotransformation of metabolites. The recirculation of the media in the chip between the
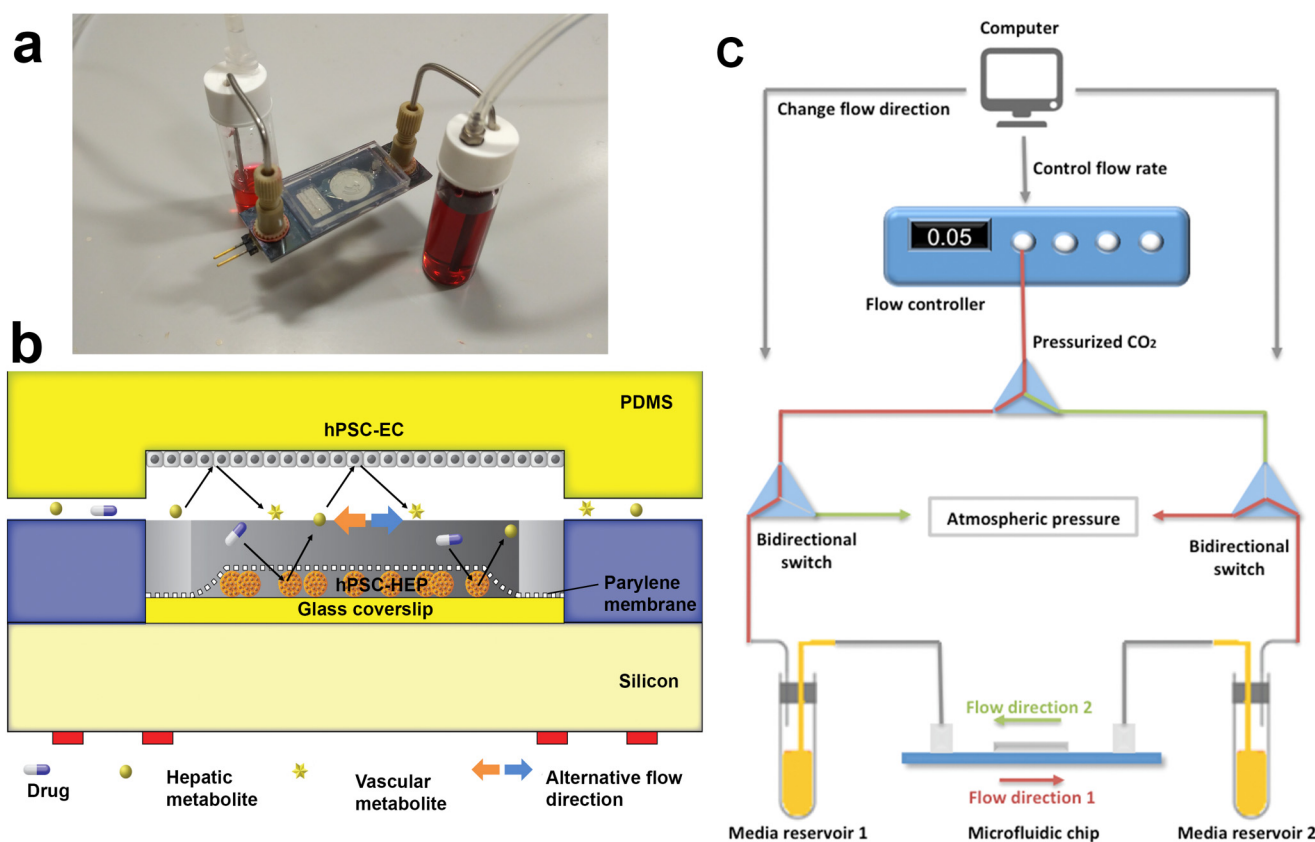

FIG. 1. Vascular-liver PIC: (a) photo of the PIC, showing the glass–silicon chip, connectors, tubing, and media reservoirs and (b) cross-section schematic of the cell co-culture chamber. (c) Schematic of the bidirectional perfusion culture testing setup. Pressurized CO_2 gas is connected to two bidirectional switches ports that control the flow direction. The computer-controlled flow controller changes flow direction every 4 h to ensure adequate time for mass transfer and biotransformation of metabolites.

two media reservoirs allow the metabolites to accumulate in the media for the detection and transformation into secondary metabolites. The media used for the perfusion culture were a 1:1 combination of EGM2 medium (hPSC-EC) and Williams E medium (hPSC-HEP).

EC cell culture and surface modification of the substrate

We used the lower side of the PDMS cover facing the cell culture chamber in our microfluidic chip [Fig. 1(b)] as the cell culture substrate for hPSC-EC. The PDMS was surface modified by 3,4-dihydroxy-L-phenylalanine (DOPA). DOPA forms strong covalent and non-covalent interaction with the surface and is a great binding agent for attachment to wet surfaces.[40] The PDMS substrates used for EC attachment were immersed in DOPA solution (2 mg/ml in 10 mM Tris, pH 8.5) overnight to improve cell attachment in the perfusion flow. We also prepared PDMS substrates with collagen I coating as a comparison. Quant-iT PicoGreen Assay (Thermo Fisher, USA) was performed to quantify the remaining cell number by the end of experiments. 10^5 cells were seeded on each perfusion culture substrate and static culture substrates.

Constrained spheroids hepatocyte cell culture and substrate

hPSC-HEPs are seeded on Polyethylene glycol (PEG)-galactose-modified glass coverslips at 1×10^5 cells/cm^2 to form spheroids. After 1 day of culture, the spheroids were immobilized with a $2\,\mu m$-thick Parylene C membrane (constrained spheroids method.[37] The hPSC-HEPs were cultured in William's E medium. Cell seeding glass coverslips (Lauda-Königshofen, Germany) are 10 mm in diameter. 1-O-(6′-aminohexyl)-D-galactopyranoside (AHG, M.W. 279), the galactose ligand for the glass surface modification was synthesized in house and verified by NMR spectrum. After 1 day of initiation in the static culture, the spheroids were moved to the chip for perfusion culture.

Real-time quantitative polymer chain reaction (qPCR)

RNA was extracted with RNeasy mini kits (Qiagen, Germany) and reverse-transcribed with cDNA synthesis kit (Bio-Rad, USA) into cDNA according to manufacturers' instructions. qPCR was performed with a 7000 Fast Real-Time PCR System (Applied Biosystems, USA). The expression levels were normalized to Glyceraldehyde 3-phosphate dehydrogenase (GAPDH) expression level to take account of different cell numbers.

Immunostaining

Cells were fixed with 4% paraformaldehyde (Sigma, USA) for 15 min and permeabilized for 3 min by 0.5% Triton X-100 (Sigma, USA) in PBS solution with Ca^{2+} and Mg^{2+}. Blocking was done overnight with PBS containing 10% serum. Cells were then incubated with PBS containing eNOS antibody (Abcam, UK) for 1 h and secondary antibody for another hour. After two washing, DAPI (Thermo Fisher, USA) was used to stain the cell nucleus for 10 min.

Urea synthesis

Urea content was measured by collecting 1 ml culture media each day and quantified with a urea nitrogen kit (Stanbio Laboratory, USA).

Cell viability staining

The viability of hPSC-EC was confirmed by a dual staining method: Propidium iodide (PI) and Calcein AM (Molecular Probes, USA). The cells were stained by incubating in $100\,\mu l$ of 25 mg/ml PI for 30 min and $1\,\mu M$ Calcein AM for 30 min.

Enzyme-linked immunosorbent assay (ELISA)

Human IL-8 in the media was quantified with a human IL-8 ELISA kit (Invitrogen, USA). Albumin was quantified with human albumin ELISA quantitation kit (Bethyl Laboratories, USA).

Liquid chromatography-mass spectrometry (LC-MS)

To test the activity of the hPSC-HEP in metabolizing the nutraceutical, the cells were exposed to $10\,\mu M$ quercetin for 72 h. The concentration of the resulting metabolites was tested against a standard with known concentration according to the methods presented in Ref. 17. The SPE column (Phenomenex, Strata C18-E, $55\,\mu m$, 70 A) was conditioned by washing with 1 ml methanol and then 2 ml de-ionized (DI) water. Conditioned media was added into the column and 1.5 ml 30% methanol was added to elute the impurity such as phenol red in the medium. 0.1% formic acid methanol was added to the column to elute all the metabolites and Internal Standard (IS) out to a 15 ml tube. The liquid in the 15 ml tube was dried under N_2 in a sample concentrator with 30 °C heater. After drying the sample, $100\,\mu l$ of 0.1% formic acid methanol was added to the 15 ml tube and vortexed for 30 s and transferred to another 1.5 ml tube. The samples were then centrifuged at 13 000 rpm for 10 min at 4 °C and $10\,\mu l$ of the supernatant was injected into LC-MS. High performance liquid chromatography combined with electrospray ionization ion trap time-of-flight multistage mass spectrometry (HPLC–DAD–ESI-IT-TOF-MSn) analyses were performed with a Shimadzu LC-MS-IT-TOF instrument, consisting of two LC-20AD pumps, an SIL-20AC autosampler, a CTO-20A column oven, a CBM-20A system controller, an ESI ion source, and an IT-TOF mass spectrometer (Shimadzu, Japan).

Statistical analysis

At least three experimental replicates were used for each data point. Statistical comparisons were conducted by Student's T-test for two groups of samples or two-way ANOVA with Bonferroni's post-hoc test in multiple group comparisons. Analyses were carried out with Graphpad Prism 6 software. Results are expressed as means ± standard error of the means (sem) of three independent experiments.

RESULTS AND DISCUSSION

Biological functions of hPSC-HEP

Liver cells lose their two-dimensional architecture gradually in standard cell culture conditions. However, under the microfluidic perfusion environment, maintenance of physiological culture
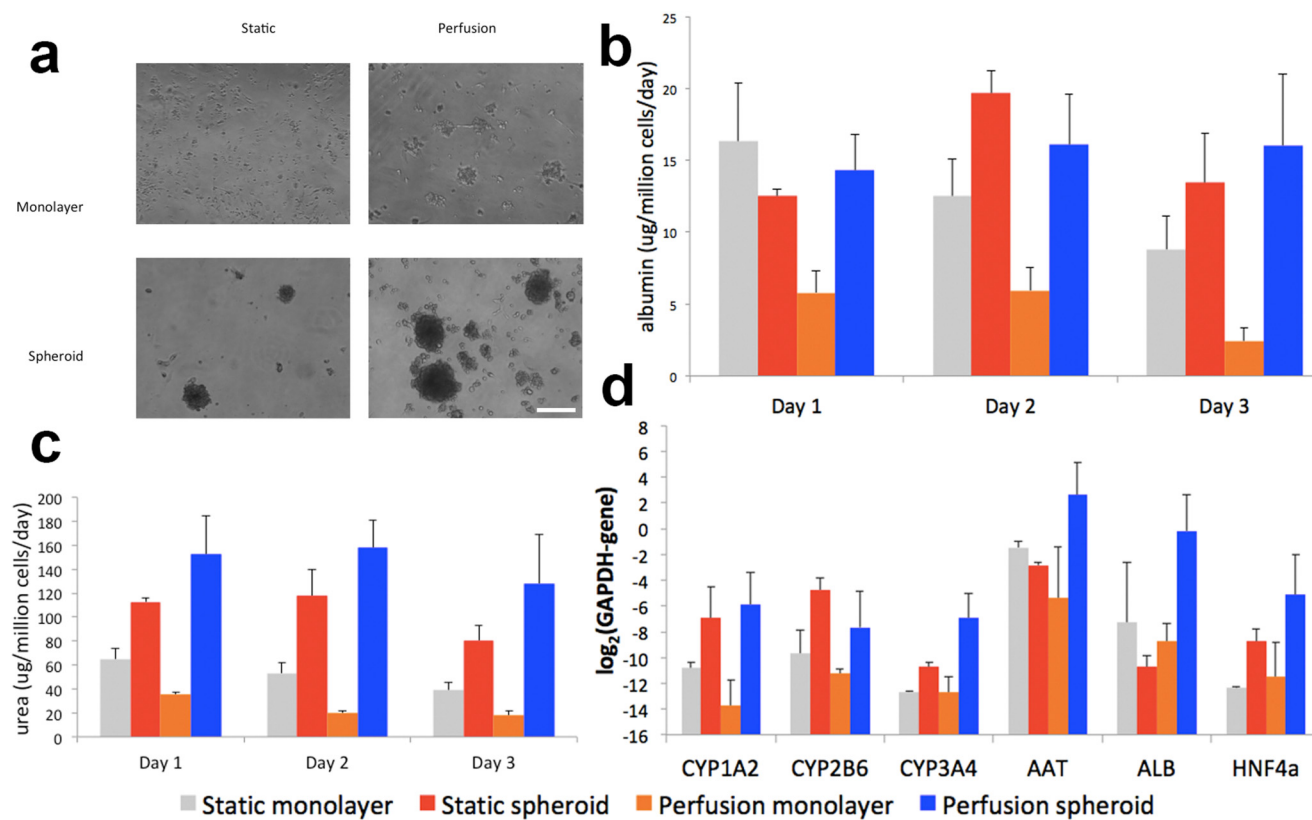
FIG. 2. Functional maintenance of the hPSC-HEP monolayer and constrained spheroids cell culture. hPSC-HEPs grows to a monolayer on the non-modified surface and form spheroids on the PEG-galactose-modified surface. hPSC-HEPs were cultured for 72 h and assessed for their hepatocyte-specific functions. (a) Phase-contrast images show that of hPSC-HEPs can remain attached under perfusion for both monolayer and spheroid configurations. Scale bar represents 100 μm. (b) Albumin secretion; (c) Urea synthesis; and (d) CYPs gene expression. All functional data were normalized to the DNA content in samples. Data are presented as means ± SEM of three biological replicates.

conditions are possible.[41] We first study the response of the hPSC-HEP under perfusion conditions and compare the constrained spheroid culture model with cell culture monolayer both models being tested under dynamic and static conditions. Following the protocol previously developed on primary rat hepatocytes,[37] hPSC-HEPs were seeded on our PEG-galactose-modified glass coverslips [Fig. 2 (a)]. Albumin secretion [Fig. 2(b)] shows similar values for the 3D culture (under perfusion or static), while for urea secretion and [Fig. 2(c)] the perfused 3D culture shows a small increment. The spheroids generated with pluripotent stem cell-derived hepatocytes show better hepatocyte-specific functions. This is in concordance with our previous observations regarding the stability of the constrained spheroids model on rat hepatocytes both under static or dynamic conditions (relevant differences between static and dynamic conditions can be noticed only after 7 days of culture). Metabolic activity was higher for perfusion cultured hepatocytes. It is also interesting that over the 3-day culture period, albumin and urea production consistently goes down for monolayer culture while it increases then decreases for both static and perfusion cultured spheroids. For monolayer culture, due to the lack of polarized clusters of hepatocytes, the viable functions of the cells are gradually lost.[42,43] On the

other hand, hepatocyte polarity is preserved in spheroids, and the cells can thrive in a more favorable 3D microenvironment. The small drop in albumin and urea production on the second day of the culture is largely due to the loss of cell viability at the peripherals of the spheroids where cell attachment is loose. The normalized functions are then restored after the first day of testing.[44] We selected a few representative genes for quantification: human CYP1A2, CYP2B6, and CYP3A4 were chosen due to their important role in drug metabolism: CYP1A2 is the second most abundant CYPs in the human body and is inducible by many of the carcinogens and aromatic hydrocarbons; CYP2B6, although only account for 5% of total CYP component, is responsible for the metabolism of more than 25% of drugs in the market; while CYP3A4 is the most abundant in human liver and responsible for the metabolism of two-thirds of all marketed drugs.[45] Albumin (ALB) and α-1-antitrypsin (AAT) genes are commonly used to identify the differentiation of stem cells toward hepatocyte lineages.[46] HNF4α encodes a transcription factor that regulates the expression of several hepatic genes in liver development.[47] Gene expression profile data of hPSC-HEPs confirmed their hepatic phenotypes with higher expressions of CYP1A2, CYP3A4, AAT, ALB, and HNF4α observed [Fig. 2(d)]. Our findings suggested
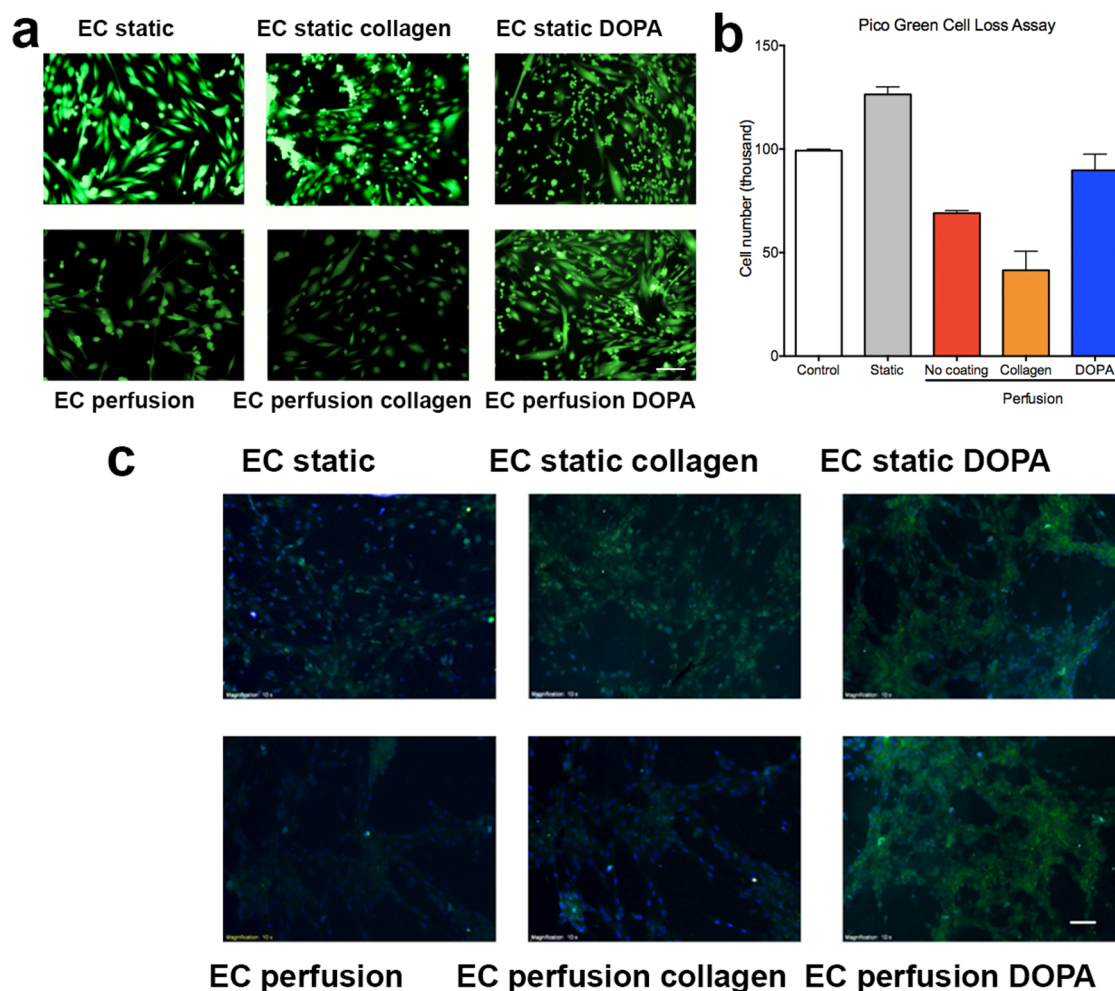
FIG. 3. (a) Live-dead staining of hPSC-EC on different substrates under static and perfusion conditions. (b) Quantification of cell attachment for different coatings. (c) Immunostaining of hPSC-EC for functional marker eNOS, nuclei are stained with DAPI. The ECs cultured under perfusion were able to express eNOS. All functional data were normalized to the DNA content in samples. Data are presented as means ± SEM of three biological replicates. Scale bar represents 100 μm.

the advantages of dynamic 3D culture in maintaining the differentiated hPSC-HEPs and enhancing their metabolic activity.

Characterization of surface coating for the hPSC-EC attachment

As a result of shear stress, cells readily detach from the surface of microfluidic devices, causing a reduction in cell number.[48] As a result, most of the surface modifications developed for cell culture under static conditions are insufficient to maintain good cell attachment under perfusion. In this report, we utilized DOPA for the surface modification of PDMS substrates to improve EC attachment. As a comparison group, we coated PDMS surfaces with collagen I (commonly used in cell seeding). In the setting of static culture, both collagen and DOPA-coated surfaces showed great

support for EC attachment and growth [Fig. 3(a)]. In the setting of perfusion culture over 3 days, we observed from live-dead staining [Fig. 3(b)] that DOPA-coated surfaces supported better attachment of the EC than collagen I-coated surfaces, where cells gradually detached due to collagen I being washed off from the surface. The PDMS substrates without any coating can maintain attachment of some EC but the cell confluency was much lower than that of DOPA-coated surfaces. Quantitative results from Pico Green assay also suggested that DOPA coating supported better cell attachment under perfusion condition, whereas non-coated and collagen I-coated surface experienced a decline in cell number. The total cell number on the DOPA-coated surface was twice that of the collagen I-coated surface. The findings confirm the DOPA coating of the PDMS surface as an effective method for the surface modification for EC culture under perfusion.
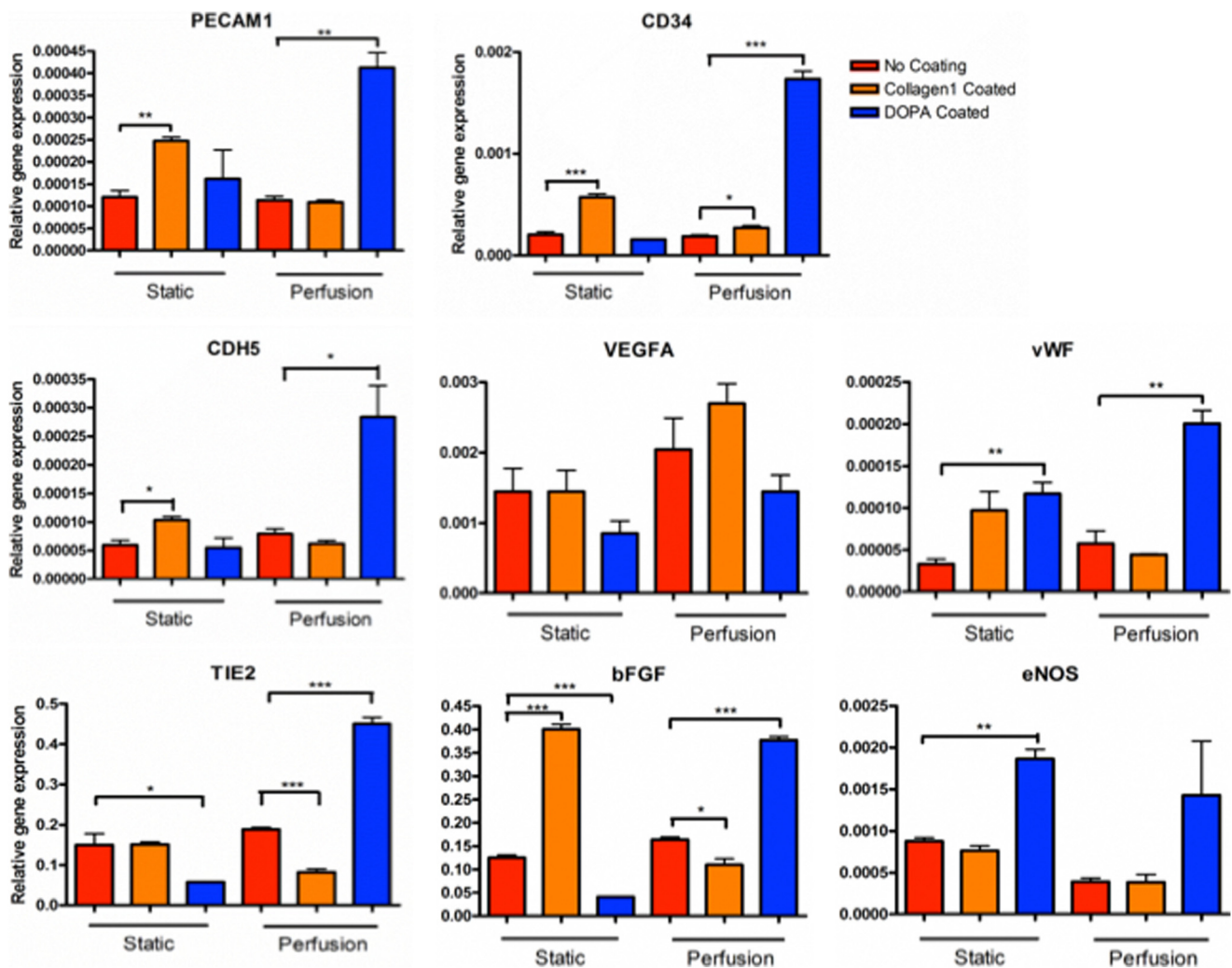
FIG. 4. Endothelial-specific gene expressions for hPSC-EC. Perfusion cultured hPSC-EC on the DOPA surface have higher gene expression compared with the control and collagen-coated surface. All functional data were normalized to the DNA content in samples. Data are presented as means ± SEM of three biological replicates.

Biological functions of hPSC-EC

Perfusion cultures have been found to improve cell functions by a considerable margin due to its enhanced delivery of nutrients and maintenance of a physiological level of fluidic shear stress.[19] Immunostaining of hPSC-EC [Fig. 3(c)] revealed that the ECs cultured under perfusion were able to express endothelial NOS (eNOS), a nitric oxide producing enzyme specifically found in vascular endothelium.[49]

Gene expression profiles of hPSC-EC (Fig. 4) also suggested the PIC system successfully maintained the stem cells' EC phenotype and improved expression of endothelium-specific genes. Significantly increased expression of PECAM1, CD34, CDH5, vWF, TIE2, βFGF, and eNOS were observed in PCR results. Elevated expression of PECAM1, a highly expressed receptor at endothelial cell–cell junctions,[50] suggested improved cell junctional integrity. CD34[51] and CDH5[52] are transmembrane glycoproteins found on blood vessels cells, they are essential adhesion molecules that promote cell attachment, the enhanced production of it shows improved cell attachment on culture surface. Von Willebrand factor (VWF) is a large glycoprotein that plays important roles in primary hemostasis,[53] the activation of it in endothelial cells shows the promotion of platelet recruitment and is a good sign of endothelial cell function. TIE2 is a receptor tyrosine kinase and has important signaling functions in developmental vascular formation.[54] Basic fibroblast growth factor (bFGF) is a modulator of cell proliferation,[55] its expression shows healthy cell attachment and proliferation in the perfusion cultured hPSC-ECs on DOPA-coated surface. The significant elevation of endothelial markers in DOPA-coated groups

is because DOPA improves the PDMS surface property for better cell attachment and proliferation. On the contrary, collagen coating was readily washed off, causing cell detachment, especially under perfusion condition.

Characterization of drug adsorption

Adsorption of proteins and large drug molecules is a challenge for microfluidic systems with high surface-to-volume-ratio.[56] Adsorption may lead to an unpredictable reduction in the drug or
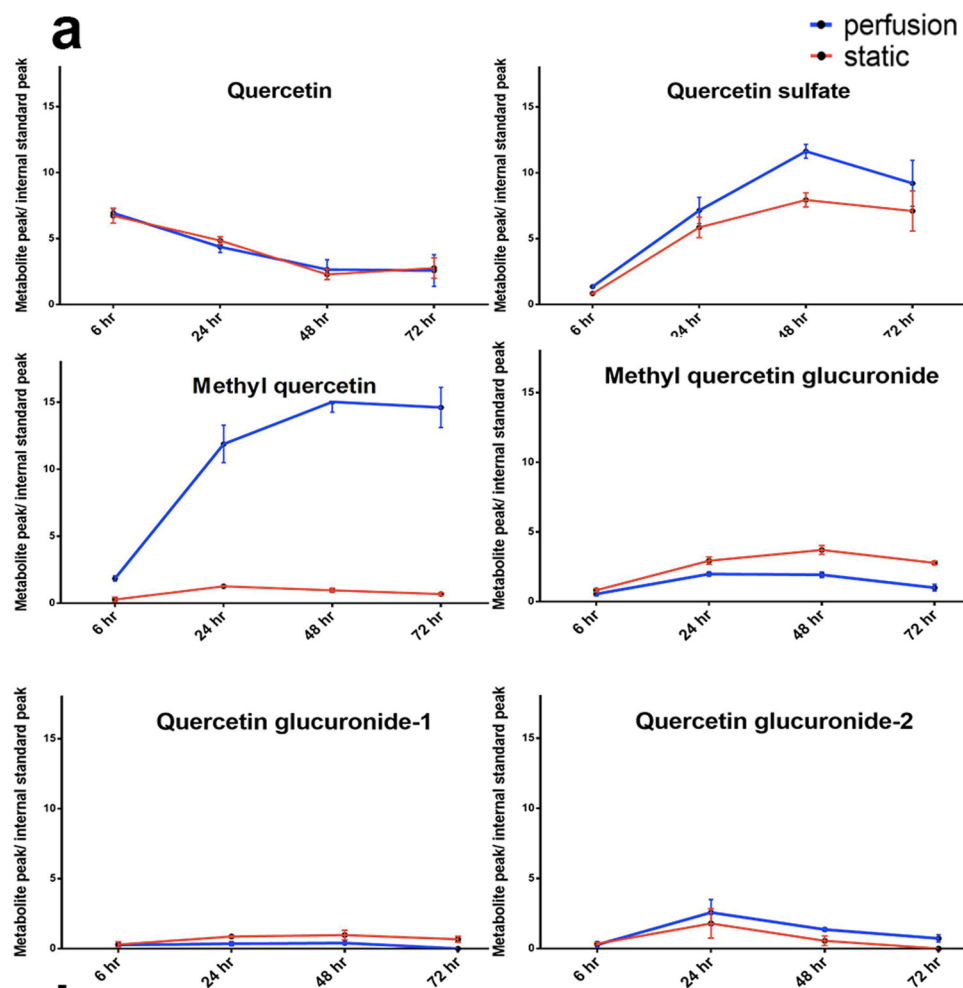

FIG. 5. LC-MS analysis of nutraceutical metabolic profiles. Perfusion co-culture produced higher levels of quercetin metabolites. IL-1β was used to activate cellular inflammation, which induced the production of IL-8. LC-MS quantification of quercetin metabolite production for (a) static cultured cells and perfusion cultured cells. (b) In the IL-8 quantification results acquired with LC-MS, perfusion culture showed more significant suppression of immune response compared with static culture. All functional data were normalized to the DNA content in samples. Data are presented as means ± SEM of three biological replicates.
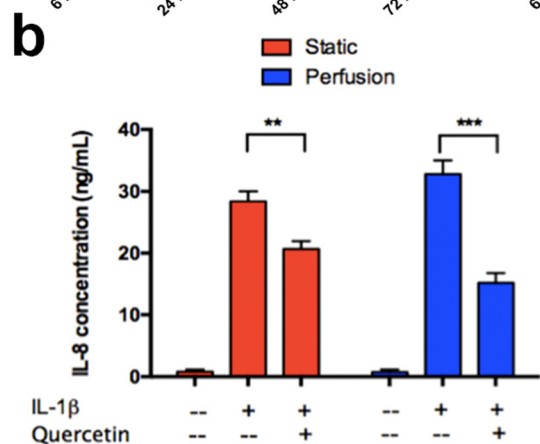
metabolite concentration[57] and can slow down the mass transfer in the perfusion culture.[58] In our application, some of the nutraceutical metabolites are very low in relative concentration, hence any reduction in their concentration due to surface adsorption may lead to inaccurate metabolite concentration results quantified by LC-MS. With a low cell seeding quantity and low metabolite concentration, it is very important to minimize the drug adsorption on the surface of the channels so we can acquire a relatively accurate measurement of the metabolite concentration. A combination of two strategies was adopted in this study. First, stainless steel tubing was adopted because of its excellent anti-fouling ability and the length of the tubing was minimized. Second, the system was passivated with BSA, to further reduce the adsorption of protein and large molecules.[39] To test the effectiveness of these approaches in our system, we flowed quercetin containing media through the system with different configurations. Results from the LC-MS measurements showed that the system utilizing stainless steel tubing and treated with BSA experienced the least drug adsorption compared with other settings (the supplementary material). The time-dependent adsorption profile also suggested that most compound adsorption happened within the first 3 h of the experiment.

Metabolism of nutraceutical

Quercetin is one of the most taken flavonoids with diet, it is useful in the reduction of oxidative stress and vasodilation of blood vessels.[59] Quercetin is metabolized in the liver, its metabolites are bioactive and present greater anti-inflammatory effects as compared with their parent compound.[60,61] Although the exact mechanism of the anti-inflammatory effect of quercetin is still not clear, it has been shown in human trials that chronic inflammation can be mitigated by quercetin consumption.[62] In this study, we selected the methylated, sulfated, and glucuronated metabolites of quercetin for quantification by LC-MS. These metabolites are formed in the hepatocytes by phase II metabolism.[59] LC-MS analysis showed that quercetin was continuously being metabolized by hPSC-HEPs [Fig. 5(a)]. The quercetin concentration depletion rate for static cultured cells and perfusion cultured cells are similar, although perfusion cultured cells expressed higher metabolic activities. This could be due to the dilution effect in the perfusion culture. In the perfusion culture, although the drug concentration was the same as static culture and we seeded the same number of cells for each experiment, the total media volume was higher than that of the static culture. Besides, the decrease in the detected quercetin concentration was contributed by the drug absorption on the microfluidic channel and tubing. The drop in the quercetin level does not fully represent the amount metabolized by the cells. The production of quercetin's metabolites was quantified. Methyl quercetin is the main quercetin metabolite, it had significantly higher concentrations in the perfusion cultured chips than static culture. This is the result of increasing biological function in perfusion culture; this also shows the effectiveness of our efforts to reduce the total media volume and the drug absorption on the surface of the microfluidic setup. For other metabolites such as the sulfated and glucuronated metabolites, the increase in concentration was not significant, because the baseline production level

of these metabolites were already very low, and they account for only less than 10% of the total quercetin metabolites.[63]

Suppression of immune response in co-culture

Inflammation is seen as the hallmark of atherosclerosis.[3] To recapitulate atherosclerosis condition, we used interleukin-1 beta (IL-1β), an inflammation cytokine, to stimulate an inflammatory response in hPSC-EC. We administered 20 ng/ml of IL-1β to the cells, this concentration was reported to be effective to induce a vascular inflammatory response.[64] As a result of the inflammation, the ECs' interleukin 8 (IL-8) production is significantly enhanced.[65] We used this mechanism to monitor the activation and suppression of inflammation in the hPSC-EC. We found that IL-8 production was much higher when hPSC-ECs were stimulated by IL-1β [Fig. 5(b)]. When quercetin was administered, a decrease of IL-8 production was observed, suggesting suppression of immune response under quercetin treatment. This confirms that hPSC-HEPs can bio-activate and transform quercetin into its active metabolites. Furthermore, the IL-8 secretion in the perfusion culture was suppressed more significantly compared with static culture. The difference could be due to enhanced biotransformation functions of the hPSC-HEPs in perfusion culture, a higher amount of active metabolite is available to suppress the inflammatory response caused by IL-1β. This gave rise to a better metabolite turnover that suppressed inflammatory activation in the hPSC-ECs.

CONCLUSIONS

We have developed an integrated alternating flow microfluidic-assisted co-culture model to study the efficacy of nutraceuticals in vascular protection. The design focused on creating an optimized microenvironment for recapitulating the endothelial-hepatic system. We modified the PDMS surface with DOPA to improve hPSC-EC attachment under perfusion. We implemented the constrained spheroid model to improve hepatocyte functions. To reduce the adsorption of drugs to microchannels and increase relative drug concentrations, we used passivated stainless steel tubing and limited the total volume of media. We studied the biotransformation of quercetin and evaluated the inflammatory suppressive effects of its metabolites. The findings suggested that the vascular-liver co-culture model is suitable for drug testing using cells with limited metabolism functions such as hPSC-derived cells. Our alternating flow co-culture platform is suitable for screening nutraceuticals and studying the biotransformation mechanisms of complex drug compounds.

SUPPLEMENTARY MATERIAL

See the supplementary material for the characterization of drug adsorption profile with silicone tubing and stainless steel tubing.

DATA AVAILABILITY

The data that support the findings of this study are available within the article.

REFERENCES

[1]C. J. Murray and A. D. Lopez, "Alternative projections of mortality and disability by cause 1990–2020: Global Burden of Disease Study," Lancet **349**, 1498–1504 (1997).

[2]K. M. Anderson, P. M. Odell, P. W. Wilson, and W. B. Kannel, "Cardiovascular disease risk profiles," Am. Heart J. **121**, 293–298 (1991).

[3]P. Libby, P. M. Ridker, and G. K. Hansson, "Progress and challenges in translating the biology of atherosclerosis," Nature **473**, 317–325 (2011).

[4]J. K. Liao and U. Laufs, "Pleiotropic effects of statins," Annu. Rev. Pharmacol. Toxicol. **45**, 89 (2005).

[5]E. K. Kalra, "Nutraceutical-definition and introduction," AAPS Pharmsci. **5**, 27–28 (2003).

[6]J. S. Cohn, E. Wat, A. Kamili, and S. Tandy, "Dietary phospholipids, hepatic lipid metabolism and cardiovascular disease," Curr. Opin. Lipidol. **19**, 257–262 (2008).

[7]D. Heber, "Herbs and atherosclerosis," Curr. Atheroscler. Rep. **3**, 93–96 (2001).

[8]C. L. K. Koide, A. C. Collier, M. J. Berry, and J. Panee, "The effect of bamboo extract on hepatic biotransforming enzymes—Findings from an obese—Diabetic mouse model," J. Ethnopharmacol. **133**, 37–45 (2011).

[9]M. J. Gómez-Lechón, J. V. Castell, and M. T. Donato, "Hepatocytes—The choice to investigate drug metabolism and toxicity in man: In vitro variability as a reflection of in vivo," Chem. Biol. Interact. **168**, 30–50 (2007).

[10]J. Yu, M. A. Vodyanik, K. Smuga-Otto, J. Antosiewicz-Bourget, J. L. Frane, S. Tian et al., "Induced pluripotent stem cell lines derived from human somatic cells," Science **318**, 1917–1920 (2007).

[11]K. Takahashi, K. Tanabe, M. Ohnuki, M. Narita, T. Ichisaka, K. Tomoda et al., "Induction of pluripotent stem cells from adult human fibroblasts by defined factors," Cell **131**, 861–872 (2007).

[12]W. J. Adams, Y. Zhang, J. Cloutier, P. Kuchimanchi, G. Newton, S. Sehrawat et al., "Functional vascular endothelium derived from human induced pluripotent stem cells," Stem Cell Rep. **1**, 105–113 (2013).

[13]C. Cheung, A. S. Bernardo, M. W. B. Trotter, R. A. Pedersen, and S. Sinha, "Generation of human vascular smooth muscle subtypes provides insight into embryological origin-dependent disease susceptibility," Nat. Biotechnol. **30**, 165–173 (2012).

[14]M. Ulvestad, P. Nordell, A. Asplund, M. Rehnström, S. Jacobsson, G. Holmgren et al., "Drug metabolizing enzyme and transporter protein profiles of hepatocytes derived from human embryonic and induced pluripotent stem cells," Biochem. Pharmacol. **86**, 691–702 (2013).

[15]C. Cheung, A. S. Bernardo, R. A. Pedersen, and S. Sinha, "Directed differentiation of embryonic origin-specific vascular smooth muscle subtypes from human pluripotent stem cells," Nat. Protoc. **9**, 929–938 (2014).

[16]F. Tasnim, D. Phan, Y.-C. Toh, and H. Yu, "Cost-effective differentiation of hepatocyte-like cells from human pluripotent stem cells using small molecules," Biomaterials **70**, 115–125 (2015).

[17]B. C. Narmada, Y. T. Goh, H. Li, S. Sinha, H. Yu, and C. Cheung, "Human stem cell-derived endothelial-hepatic platform for efficacy testing of vascular-protective metabolites from nutraceuticals," Stem Cells Transl. Med. **6**, 851–863 (2017).

[18]S. N. Bhatia and D. E. Ingber, "Microfluidic organs-on-chips," Nat. Biotechnol. **32**, 760–772 (2014).

[19]D. Huh, G. A. Hamilton, and D. E. Ingber, "From 3D cell culture to organs-on-chips," Trends Cell Biol. **21**, 745–754 (2011).

[20]F. Yu, F. S. Iliescu, and C. Iliescu, "A comprehensive review on perfusion cell culture systems," Inform. MIDEM **46**, 163–175 (2016).

[21]E. Jastrzębska, U. Bazylińska, M. Bułka, K. Tokarska, M. Chudy, A. Dybko et al., "Microfluidic platform for photodynamic therapy cytotoxicity analysis of nanoencapsulated indocyanine-type photosensitizers," Biomicrofluidics **10**, 014116 (2016).

[22]F. S. Iliescu, D. P. Poenar, F. Yu, M. Ni, K. H. Chan, I. Cima et al., "Recent advances in microfluidic methods in cancer liquid biopsy," Biomicrofluidics **13**, 041503 (2019).

[23]F. Yu and D. Choudhury, "Microfluidic bioprinting for organ-on-a-chip models," Drug Discov. Today **23**(4), 815–829 (2019).

[24]F. Yu, N. D. Selva Kumar, D. Choudhury, L. C. Foo, and S. H. Ng, "Microfluidic platforms for modeling biological barriers in the circulatory system," Drug Discov. Today **10**(6), 1248–1256 (2018).

[25]H. Jiang, D. Jiang, P. Zhu, F. Pi, J. Ji, C. Sun et al., "A novel mast cell co-culture microfluidic chip for the electrochemical evaluation of food allergen," Biosens. Bioelectron. **83**, 126–133 (2016).

[26]M. B. Esch, H. Ueno, D. R. Applegate, and M. L. Shuler, "Modular, pumpless body-on-a-chip platform for the co-culture of GI tract epithelium and 3D primary liver tissue," Lab Chip **16**, 2719–2729 (2016).

[27]E. M. Materne, A. P. Ramme, A. P. Terrasso, M. Serra, P. M. Alves, C. Brito et al., "A multi-organ chip co-culture of neurospheres and liver equivalents for long-term substance testing," J. Biotechnol. **205**, 36–46 (2015).

[28]I. Wagner, E. M. Materne, S. Brincker, U. Sussbier, C. Fradrich, M. Busek et al., "A dynamic multi-organ-chip for long-term cultivation and substance testing proven by 3D human liver and skin tissue co-culture," Lab Chip **13**, 3538–3547 (2013).

[29]F. Yu, S. Zhuo, Y. Qu, D. Choudhury, Z. Wang, C. Iliescu et al., "On chip two-photon metabolic imaging for drug toxicity testing," Biomicrofluidics **11**, 034108 (2017).

[30]I. Maschmeyer, A. K. Lorenz, K. Schimek, T. Hasenberg, A. P. Ramme, J. Hubner et al., "A four-organ-chip for interconnected long-term co-culture of human intestine, liver, skin and kidney equivalents," Lab Chip **15**, 2688–2699 (2015).

[31]I. Maschmeyer, T. Hasenberg, A. Jaenicke, M. Lindner, A. K. Lorenz, J. Zech et al., "Chip-based human liver-intestine and liver-skin co-cultures—A first step toward systemic repeated dose substance testing in vitro," Eur. J. Pharm. Biopharm. **95**, 77–87 (2015).

[32]J. M. Prot, L. Maciel, T. Bricks, F. Merlier, J. Cotton, P. Paullier et al., "First pass intestinal and liver metabolism of paracetamol in a microfluidic platform coupled with a mathematical modeling as a means of evaluating ADME processes in humans," Biotechnol. Bioeng. **111**, 2027–2040 (2014).

[33]G. J. Mahler, M. B. Esch, R. P. Glahn, and M. L. Shuler, "Characterization of a gastrointestinal tract microscale cell culture analog used to predict drug toxicity," Biotechnol. Bioeng. **104**, 193–205 (2009).

[34]D. Choudhury, X. Mo, C. Iliescu, L. L. Tan, W. H. Tong, and H. Yu, "Exploitation of physical and chemical constraints for three-dimensional microtissue construction in microfluidics," Biomicrofluidics **5**, 022203 (2011).

[35]U. Marx, H. Walles, S. Hoffmann, G. Lindner, R. Horland, F. Sonntag et al., "Human-on-a-chip' developments: A translational cutting-edge alternative to systemic safety assessment and efficiency evaluation of substances in laboratory animals and man?," Altern. Lab. Anim. **40**, 235 (2012).

[36]F. Yu, R. Deng, W. H. Tong, L. Huan, N. C. Way, A. IslamBadhan et al., "A perfusion incubator liver chip for 3D cell culture with application on chronic hepatotoxicity testing," Sci. Rep. **7**, 14528 (2017).

[37]W. H. Tong, Y. Fang, J. Yan, X. Hong, N. H. Singh, S. R. Wang et al., "Constrained spheroids for prolonged hepatocyte culture," Biomaterials **80**, 106–120 (2016).

[38]A. J. Sedriks, Corrosion of Stainless Steel, 2nd ed. (Wiley, 1996).

[39]C. Zhang, J. Xu, W. Ma, and W. Zheng, "PCR microfluidic devices for DNA amplification," Biotechnol. Adv. **24**, 243–284 (2006).

[40]H. Lee, S. M. Dellatore, W. M. Miller, and P. B. Messersmith, "Mussel-inspired surface chemistry for multifunctional coatings," Science **318**, 426–430 (2007).

[41]S. Zhang, W. Tong, B. Zheng, T. A. Susanto, L. Xia, C. Zhang et al., "A robust high-throughput sandwich cell-based drug screening platform," Biomaterials **32**, 1229–1241 (2011).

[42]Z. Jia, Y. Cheng, X. Jiang, C. Zhang, G. Wang, J. Xu *et al.*, "3D culture system for liver tissue mimicking hepatic plates for improvement of human hepatocyte (C3A) function and polarity," BioMed Res. Int. **2020**, 6354183 (2020).

[43]A. Treyer and A. Musch, "Hepatocyte polarity," Compr. Physiol. **3**, 243–287 (2013).

[44]C. C. Bell, D. F. G. Hendriks, S. M. L. Moro, E. Ellis, J. Walsh, A. Renblom *et al.*, "Characterization of primary human hepatocyte spheroids as a model system for drug-induced liver injury, liver function and disease," Sci. Rep. **6**, 25187 (2016).

[45]S. Rendic, "Summary of information on human CYP enzymes: Human P450 metabolism data," Drug Metab. Rev. **34**, 83–448 (2002).

[46]P. Huang, L. Zhang, Y. Gao, Z. He, D. Yao, Z. Wu *et al.*, "Direct reprogramming of human fibroblasts to functional and expandable hepatocytes," Cell Stem Cell **14**, 370–384 (2014).

[47]C. Walesky and U. Apte, "Role of hepatocyte nuclear factor 4alpha (HNF4alpha) in cell proliferation and cancer," Gene Express. **16**, 101–108 (2015).

[48]H. Lu, L. Y. Koo, W. M. Wang, D. A. Lauffenburger, L. G. Griffith, and K. F. Jensen, "Microfluidic shear devices for quantitative analysis of cell adhesion," Anal. Chem. **76**, 5257–5264 (2004).

[49]J. E. Fish and P. A. Marsden, "Endothelial nitric oxide synthase: Insight into cell-specific gene regulation in the vascular endothelium," Cell. Mol. Life Sci. **63**, 144–162 (2006).

[50]P. Lertkiatmongkol, D. Liao, H. Mei, Y. Hu, and P. J. Newman, "Endothelial functions of platelet/endothelial cell adhesion molecule-1 (CD31)," Curr. Opin. Hematol. **23**, 253–259 (2016).

[51]A. R. Mackie and D. W. Losordo, "CD34-positive stem cells: In the treatment of heart and vascular disease in human beings," Tex. Heart Inst. J. **38**, 474–485 (2011).

[52]X. G. Mao, X. Y. Xue, L. Wang, X. Zhang, M. Yan, Y. Y. Tu *et al.*, "CDH5 is specifically activated in glioblastoma stemlike cells and contributes to vasculogenic mimicry induced by hypoxia," Neuro Oncol. **15**, 865–879 (2013).

[53]F. Peyvandi, I. Garagiola, and L. Baronciani, "Role of von Willebrand factor in the haemostasis," Blood Transfus. **9**(Suppl. 2), s3–s8 (2011).

[54]S. Fukuhara, K. Sako, T. Minami, K. Noda, H. Z. Kim, T. Kodama *et al.*, "Differential function of Tie2 at cell-cell contacts and cell-substratum contacts regulated by angiopoietin-1," Nat. Cell Biol. **10**, 513–526 (2008).

[55]S. I. Zittermann and A. C. Issekutz, "Basic fibroblast growth factor (bFGF, FGF-2) potentiates leukocyte recruitment to inflammation by enhancing endothelial adhesion molecule expression," Am. J. Pathol. **168**, 835–846 (2006).

[56]A. Lionello, J. Josserand, H. Jensen, and H. H. Girault, "Protein adsorption in static microsystems: Effect of the surface to volume ratio," Lab Chip **5**, 254–260 (2005).

[57]V. Linder, E. Verpoorte, W. Thormann, N. F. de Rooij, and H. Sigrist, "Surface biopassivation of replicated poly (dimethylsiloxane) microfluidic channels and application to heterogeneous immunoreaction with on-chip fluorescence detection," Anal. Chem. **73**, 4181–4189 (2001).

[58]M. S. Munson, M. S. Hasenbank, E. Fu, and P. Yager, "Suppression of nonspecific adsorption using sheath flow," Lab Chip **4**, 438–445 (2004).

[59]H. G. Ulusoy and N. Sanlier, "A minireview of quercetin: From its metabolism to possible mechanisms of its biological activities," Crit. Rev. Food Sci. Nutr. (published online 2019).

[60]H. van der Woude, M. G. Boersma, J. Vervoort, and I. M. Rietjens, "Identification of 14 quercetin phase II mono-and mixed conjugates and their formation by rat and human phase II in vitro model systems," Chem. Res. Toxicol. **17**, 1520–1530 (2004).

[61]A. V. Anand David, R. Arulmoli, and S. Parasuraman, "Overviews of biological importance of quercetin: A bioactive flavonoid," Pharmacogn. Rev. **10**, 84–89 (2016).

[62]Q. Ou, Z. Zheng, Y. Zhao, and W. Lin, "Impact of quercetin on systemic levels of inflammation: A meta-analysis of randomised controlled human trials," Int. J. Food Sci. Nutr. **71**, 152–163 (2020).

[63]Y. Li, J. Yao, C. Han, J. Yang, M. T. Chaudhry, S. Wang *et al.*, "Quercetin, inflammation and immunity," Nutrients **8**, 167 (2016).

[64]G. V. Chaitanya, W. Cromer, S. Wells, M. Jennings, J. M. Mathis, A. Minagar *et al.*, "Metabolic modulation of cytokine-induced brain endothelial adhesion molecule expression," Microcirculation **19**, 155–165 (2012).

[65]O. Cromwell, Q. Hamid, C. Corrigan, J. Barkans, Q. Meng, P. Collins *et al.*, "Expression and generation of interleukin-8, IL-6 and granulocyte-macrophage colony-stimulating factor by bronchial epithelial cells and enhancement by IL-1 beta and tumour necrosis factor-alpha," Immunology **77**, 330 (1992).